J Mater Sci: Mater Med (2008) 19:2137–2144
DOI 10.1007/s10856-007-3138-y

Electrochemical characterization of AISI 316L stainless steel in contact with simulated body fluid under infection conditions

Danián Alejandro López · Alicia Durán · Silvia Marcela Ceré

Received: 1 August 2005 / Accepted: 31 July 2006 / Published online: 13 November 2007

Abstract Titanium and cobalt alloys, as well as some stainless steels, are among the most frequently used materials in orthopaedic surgery. In industrialized countries, stainless steel devices are used only for temporary implants due to their lower corrosion resistance in physiologic media when compared to other alloys. However, due to economical reasons, the use of stainless steel alloys for permanent implants is very common in developing countries. The implantation of foreign bodies is sometimes necessary in the modern medical practice. However, the complex interactions between the host and the can implant weaken the local immune system, increasing the risk of infections. Therefore, it is necessary to further study these materials as well as the characteristics of the superficial film formed in physiologic media in infection conditions in order to control their potential toxicity due to the release of metallic ions in the human body. This work presents a study of the superficial composition and the corrosion resistance of AISI 316L stainless steel and the influence of its main alloying elements when they are exposed to an acidic solution that simulates the change of pH that occurs when an infection develops. Aerated simulated body fluid (SBF) was employed as working solution at 37 °C. The pH was adjusted to 7.25 and 4 in order to reproduce normal body and disease state respectively. Corrosion resistance was measured by means of electrochemical impedance spectroscopy (EIS) and anodic polarization curves.

D. A. López (✉) · S. M. Ceré
Instituto de Investigaciones en Ciencia y Tecnología de Materiales (INTEMA), UNMdP-CONICET, Juan B. Justo 4302, B7608FDQ Mar del Plata, Argentina
e-mail: dalopez@mdp.edu.ar

S. M. Ceré
e-mail: smcere@fi.mdp.edu.ar

A. Durán
Instituto de Cerámica y Vidrio, CSIC, Campus de Cantoblanco, 28049 Madrid, Spain
e-mail: aduran@icv.csic.es

Introduction

The use of metals in biomedical orthopaedic and dental implants is mainly based in the extreme mechanical requirements that they have when they are placed in service [1]. If possible, a metallic implant should be completely inert in the human body, but unfortunately this rarely occurs. Organic fluids are extremely hostile to metallic materials and their effect on the implants and the surrounding tissue is a matter of great importance. Although these materials have a thermodynamic tendency to corrode, they also have in common the formation of a protective film which is capable of maintaining the corrosion levels within acceptable values for practical applications, particularly when considering that the corrosion products might be toxic for the surrounding tissues. Superficial films usually have different compositions and chemical states when compared to the base material [2]. Surface characterization of the alloys employed in orthopaedic surgery should not be underestimated because of its great influence in the performance of the implant through the interaction film-tissue, and the possible migration of metallic ions from the base metal to the surrounding tissues. The efficiency of the superficial film depends on the resistance of the passivation layers to rupture and the re-passivation capability of the materials under study in the immersion media. The use of metals in orthopaedic surgery is also conditioned by the aggressivity of the physiologic medium and can lead to the

liberation of corrosion and/or wear products into the body [3–5].

Despite the numerous advances in orthopaedic surgery, the materials employed are far from being a perfect answer to the problems mentioned above. In general stainless steels alloys are employed worldwide for temporary implants whereas Co–Cr and Ti alloys are used for permanent implants.

Stainless steel is used substantially in developing countries as it is the most economic option among the metallic alloys employed in orthopaedic surgery. However, adverse responses have been found in the surrounding tissues of the implant presenting encapsulation and fibrous membranes around the prosthesis, besides the numerous failures in the head neck area of the conic coupling devices [6]. It is important to note that the composition of the protective oxides is also related to the corrosion behaviour of these biomedical implants. Thus, it is necessary to characterize in detail these surfaces in order to improve the biocompatibility of the alloys employed in surgical implants. In spite of the good properties of the passivating alloys, they can still generate metal ions which can diffuse through the passive oxide films. When in an aqueous media, they can form hydroxides or oxides, producing a local change in the pH. Furthermore, immediately after implantation, the alloy are surrounded by fibrin and chlorine ions, decreasing the local pH, possibly leading to the acceleration of the corrosion process. In turn, the decrease in pH can also be associated with infections [7]. Although the corrosion behaviour of AISI 316L has been widely studied in many conditions, there are still many aspects related to the metal response in acidic media that simulates infection condition that need to be addressed.

This work presents the electrochemical study of stainless steel AISI 316L and its main compositional elements (Fe, Cr and Ni) in contact with simulated body fluid (SBF) at 37 °C. Environmental conditions were established in order to reproduce normal exposure to human body conditions (pH 7.25) and, with the aim of characterizing the changes that possibly occurs in the event of an infection, alloys were also tested in SBF acidic solution (pH 4) in order to simulate the acidic media and the high chloride concentrations that develop when disease conditions are present [7]. The electrochemical behaviour for each material was evaluated by potentiodynamic polarization and electrochemical impedance spectroscopy (EIS) after an immersion time of 24 h.

Experimental

The tests were conducted employing stainless steel AISI 316L (wt.%: 17–20 Cr, 12–14 Ni, 2–4 Mo, 2 max. Mn, 0.75 max. Si, 0.03 max. S, 0.03 max. P, 0.03 max. C, Fe balance [8]) and its main alloy components: Fe, Cr and Ni (99.9 wt.% purity). The electrodes were built from discs obtained from rods of the respective materials, which were included in PVC holders and filled with an epoxy resin. The electrical contacts were made by means of a wire welded in the rear part of the working material before sealing it with the aforementioned epoxy resin. The samples were then polished with emery paper up to grit 600.

In the case of AISI 316L samples, a previous treatment was performed in order to avoid crevice corrosion. The side of the discs were polished with emery paper grit 240 and then they were passivated in a 50% vol. nitric acid solution at 50 °C for 30 min. Afterwards, the sides were painted with a thermo-cured phenolic epoxy lacquer (B5061/F Synco^{TM}) and treated in an oven at 120 °C for 10 min.

For the tests conducted at pH 7.25 ± 0.05 the SBF was prepared with the following chemical composition [9]: NaCl (8.053 g L^{-1}), KCl (0.224 g L^{-1}), $CaCl_2$ (0.278 g L^{-1}), $MgCl_2.6H_2O$ (0.305 g L^{-1}), K_2HPO_4 (0.174 g L^{-1}), $NaHCO_3$ (0.353 g L^{-1}), $(CH_2OH)_3CNH_2$ (6.057 g L^{-1}). On the other hand, the acidic SBF (pH 4 ± 0.05) was prepared as follows [9]: NaCl (8.053 g L^{-1}), KCl (0.224 g L^{-1}), $CaCl_2$ (0.278 g L^{-1}), $MgCl_2.6H_2O$ (0.305 g L^{-1}), K_2HPO_4 (0.174 g L^{-1}), $NaHCO_3$ (0.353 g L^{-1}), $C_6H_4(COOK)(COOH)$ (10.200 g L^{-1}). In both cases the final pH value was reached with the addition of concentrated HCl.

The electrochemical measurements were done with a Solartron 1280B unit using a three electrodes cell, with a Pt counterelectrode and a saturated calomel electrode (SCE) as reference. A thermostatic bath (Vicking 4100) was employed to keep the temperature at 37 °C. The samples were preconditioned in aerated SBF during 24 h previous to the electrochemical essays, without bubbling during the realization of the tests.

Anodic polarization curves were obtained by means of a potentiodynamic sweep from the corrosion potential (E_{corr}) up to a value of 0.5 V vs. SCE or a current density of 0.001 A cm^{-2}. The sweep rate was 0.001 v s^{-1}. EIS spectra were collected modulating 0.005 V rms in a frequency range of 20000 Hz to 0.01 Hz. Impedance fitting was performed using Zplot software [10]. On the other hand, E_{corr} was monitored before and after the electrochemical tests mentioned above.

Results and discussion

Corrosion potential (E_{corr})

Table 1 shows the average values of E_{corr} observed for each material immersed for 24 h in aerated SBF at 37 °C, at pH 7.25 and 4 respectively.

Table 1 E_{corr} (mV vs. SCE) of the studied materials immersed in aerated SBF at 37 °C

	AISI 316LL	Cr	Ni	Fe
pH 7.25	−190 ± 40	−640 ± 40	−195 ± 65	−620 ± 5
pH 4	−120 ± 25	−505 ± 35	−200 ± 25	−620 ± 15

In both pH conditions it can be seen that the stainless steel has corrosion potentials significantly more noble than Cr and Fe, which present more negative values. However, Ni has a corrosion potential close to the values of the alloy. The values of the measured E_{corr} are consistent with other studies of the passivity of various stainless steels [11]. When the materials are tested in infection conditions, there is a slight change in the E_{corr} to more positive values for the alloy and for Cr. On the other hand, the values registered for Ni and Fe are almost the same than those observed at pH 7.25.

Polarization curves

Figures 1 and 2 display the anodic polarization curves for each material in the experimental conditions studied at pH 7.25 and 4, respectively.

The current density of Cr appears to be proportional to that of the stainless steel at both pH conditions. This is in agreement with previous reports chomium oxides are the main components in the passive film formed on these alloys [1, 11, 12], and thus, responsible for the passive behaviour of the alloy [13].

However, in the range of potentials studied, Cr does not show any evidence of pitting corrosion whereas the stainless steel does. As a consequence, oxides from the other components might influence the behaviour of the alloy, which could lead to the presence of the pitting potential observed in the stainless steel in the experimental conditions tested.

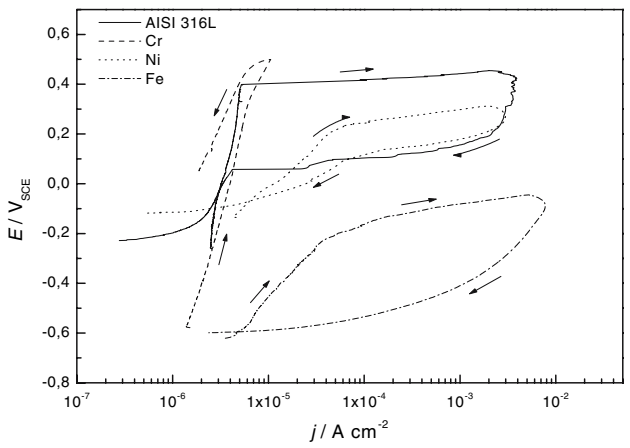

Fig. 1 Polarization curves for AISI 316L stainless steel, Cr, Ni and Fe immersed for 24 h in aerated SBF at 37 °C at pH 7.25

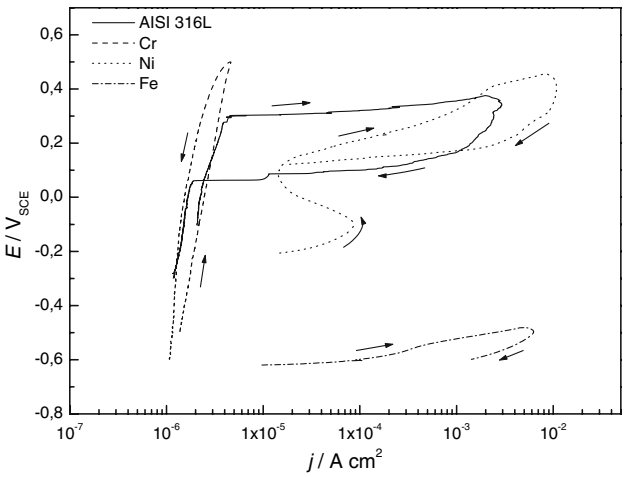

Fig. 2 Polarization curves for AISI 316L stainless steel, Cr, Ni and Fe immersed for 24 h in aerated SBF at 37 °C at pH 4

In neutral to alkaline solutions the films are usually composed of a chromium-rich inner layer and an iron-rich outer layer. In these conditions the passive film thickens basically because iron oxides are more stable in alkaline solutions. On the other hand, in acidic solutions a chromium-rich oxide film is formed due to the slower dissolution of Cr oxides compared to Fe oxides [14].

At pH 4, Ni and Fe present active dissolution and density currents of one order of magnitude higher than the alloy and Cr. As a consequence, it would be expected that under infection conditions these first components would react preferentially, releasing their corrosion products to the surrounding tissue [15, 16].

Considering their equilibrium potentials, Fe and Cr have more negative values indicating a higher activity of these elements compared to the stainless steel and Ni. However, there is little Cr found in the surrounding tissues due to ions release from the implant alloys [16]. Iron easily oxidizes in aerated solutions to Fe^{3+} and afterwards hydrolyzes into hydroxides in a broad pH range from acidic to alkaline conditions. Despite the fact that the ionic radius of Fe^{3+} is similar to that of Cr^{3+}, they differ significantly in their solution behaviour due to their electronic properties. Both exist in solution as hexa-aquocomplexes, although Cr^{3+} ions are very stable compared to Fe^{3+}. Thus, chromium (III) compounds are almost inert whereas iron (III) ones are very reactive.

The potentiodynamic tests show that chromium forms superficial oxides that are passivating while iron generates corrosion products that are not protective, leading to an active corrosion process.

On the other hand, nickel has a lower thermodynamic tendency to corrosion. In neutral to alkaline media it forms hydroxides whilst in acidic media the cation Ni^{2+} is stable in solution. That is probably why the ion release analyses

show that the relative amounts of Ni are higher than that of Cr in a pH range from 4 to 7 [16].

Electrochemical impedance spectroscopy (EIS)

AISI 316L stainless steel

Figure 3 shows the EIS Bode diagrams for the AISI 316L stainless steel after 24 h of immersion in SBF at 37 °C at pH 7.25 and 4.

The change in the impedance response suggests a non-ideal dielectric capacitive behaviour, which can be modelled by a Randles circuit with a constant phase element (CPE) (see insert in Fig. 3). A CPE can be described by the expression [10]:

$$Z_{\mathrm{CPE}} = \frac{1}{Y_0(j\omega)^n} \tag{1}$$

with $-1 < \mathrm{N} < 1$. In this equation, n is a coefficient associated to system homogeneity (where $n = 1$ for an ideal capacitor), ω is the frequency, and Y_0 is the pseudo capacitance of the system. The corresponding fitted parameters are shown in Table 2.

Two time constants in the impedance diagrams for the alloy would be expected, one corresponding to the passive film and the other to the charge transfer process in the metal surface. However, only one is clearly recognized. In order to understand this behaviour, it is necessary to analyze the parameters obtained from the fitting model. The pseudo capacitances have values that could be assigned both to the charge transfer process and to the presence of a thin or porous film. On the other hand, as the superficial film presents passivating properties, it would be expected that its resistance has similar values than the one associated to a charge transfer resistance process. As a consequence, the time constants for each of these processes are very close and their determination from the impedance spectra is quite difficult [17].

There is not much variation in the results observed for the different pH conditions for the AISI 316L stainless steel. However, a slight drop in the phase angle is evident at low frequencies at pH 4.This is consistent with the lower values of R and the increase in Y_0 in acidic conditions, denoting a lower performance in the corrosion resistance of the alloy.

Chromium

Figure 5 shows the EIS Bode diagrams for chromium after 24 h of immersion in SBF at 37 °C, at pH 7.25 and 4. The equivalent circuit employed to model the system parameters is presented in as an insert in Figure 4 and the corresponding fitting results are given in Table 3.

Two time constants are clearly derived from the Bode plots. The one at higher frequencies could be related to a

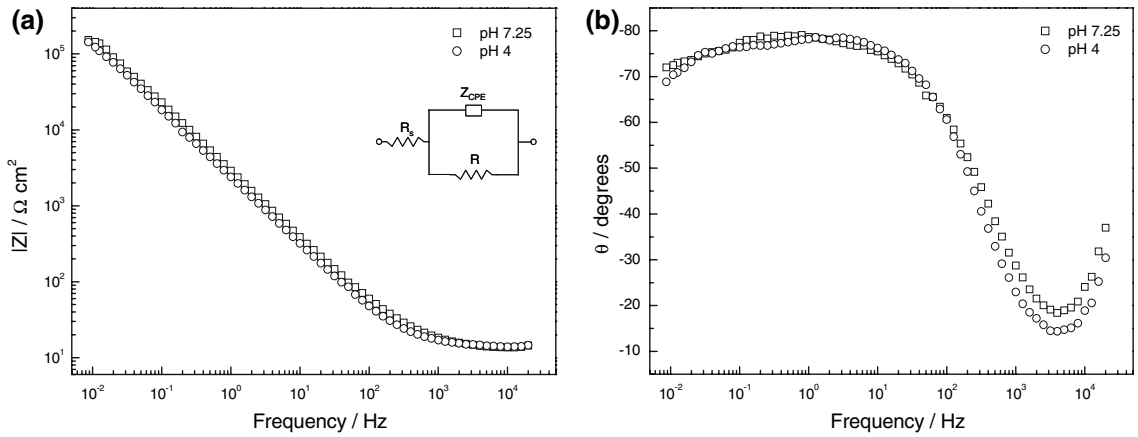

Fig. 3 EIS Bode diagrams for AISI 316L stainless steel immersed 24 h in aerated SBF at 37 °C at pH 7.25 and 4. (**a**) |Z| vs. Frequency, (**b**) θ vs. Frequency. In the insert: Equivalent electric circuit employed to model the impedance data of AISI 316L stainless steel

Table 2 Circuit parameters for AISI 316L stainless steel immersed in aerated SBF for 24 h at pH 7.25 and 4

	pH 7.25	pH 4
R_s (Ω cm^2)	15 ± 0.3	15 ± 0.3
Y_0 (Ω^{-1} cm^{-2} s^n)	$6.95 \times 10^{-5} \pm 7.64 \times 10^{-7}$	$8.25 \times 10^{-5} \pm 9.31 \times 10^{-7}$
n	$0.86 \pm 2.6 \times 10^{-3}$	$0.87 \pm 2.8 \times 10^{-3}$
R (Ω cm^2)	$1.44 \times 10^6 \pm 5.51 \times 10^5$	$5.44 \times 10^5 \pm 7.53 \times 10^4$

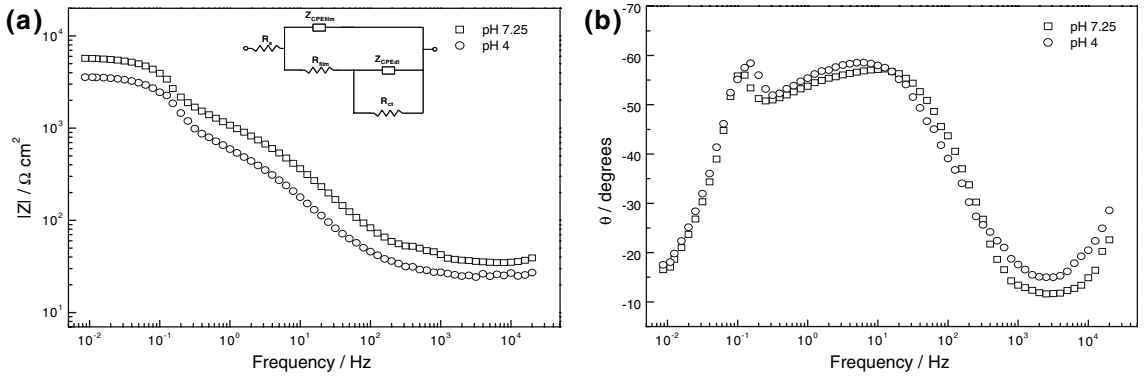

Fig. 4 EIS Bode diagrams for chromium immersed 24 h in aerated SBF at 37 °C at pH 7.25 and 4. (**a**) |Z| vs. Frequency, (**b**) θ vs. Frequency. In the insert: equivalent electric circuit employed to model the impedance data of chromium

Table 3 Circuit parameters for chromium immersed in aerated SBF for 24 h at pH 7.25 and 4

	pH 7.25	pH 4
R_s (Ω cm^2)	35 ± 1.85	35 ± 0.87
Y_{0film} (Ω^{-1} cm^{-2} s^n)	1.44 × 10^{-4} ± 1.77 × 10^{-5}	1.46 × 10^{-4} ± 3.36 × 10^{-5}
n_{film}	0.73 ± 2.29 × 10^{-2}	0.88 ± 4.06 × 10^{-2}
R_{film} (Ω cm^2)	1973 ± 332.28	525.3 ± 134.43
Y_{0dl} (Ω^{-1} cm^{-2} s^n)	3.06 × 10^{-4} ± 3.35 × 10^{-5}	4.51 10^{-4} ± 4.07 × 10^{-5}
n	0.94 ± 8.77 × 10^{-2}	0.84 ± 6.59 × 10^{-2}
R_{ct} (Ω cm^2)	5265 ± 457.18	4078 ± 401.89

chromium-oxide layer while the other at lower frequencies could be associated with the faradic processes taking place on the metal surface. There are no major differences in the impedance spectra for the two pH conditions. However, a decrease in the values of R_{film} and R_{ct} is observed in acidic conditions. Thus far, the pseudo capacitance values are similar for both pH conditions. The later could be related to a double effect of thinning and coverage of the oxide film, all produced by the degradation of the oxide layer in infection conditions.

It is worth noting that higher values of resistance would be expected considering the passive behaviour of chromium, as seen in the anodic polarization curves. Instead, the results observed from the EIS tests show values three orders of magnitude smaller than the ones obtained with the stainless steel samples. This could be explained considering that during the potentiodynamic tests the increase in the potential shifts the material towards a passive condition, thus forcing the growth of chromium-oxides. On the other hand, in the EIS tests the measurements are conducted near E_{corr}, where these oxides do not cover completely the inhomogeneous and porous original surface of the pure metal (Fig. 5).

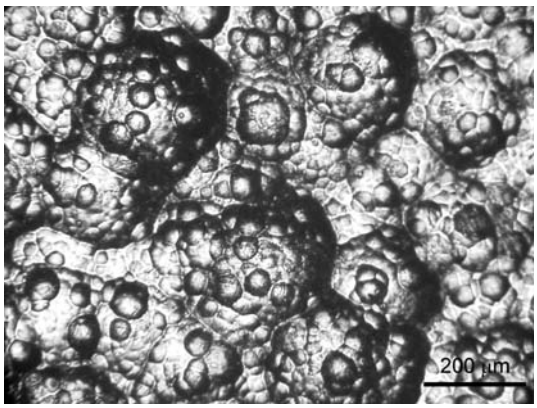

Fig. 5 Microstructure of pure chromium previous to immersion in SBF

Nickel

The EIS Bode diagrams for nickel after 24 h of immersion in SBF at 37 °C at pH 7.25 and 4 are shown in Fig. 6. It is evident that the behaviour of the metal changes radically in each pH condition, with a diffusion process taking place at acidic conditions. The Warburg impedance is used to model the increasing ionic conductivity due to corrosion process occurring in the pores and increasing diffusivity into the pores. It can be described by the equation [10]:

$$Z_w = \frac{R_{DO}}{(jT\omega)^{n_d}} \tanh\,(jT\omega)^{n_d} \qquad (2)$$

where R_{DO} is associated with the solid phase diffusion and T is related to the diffusion coefficient and the pores length.

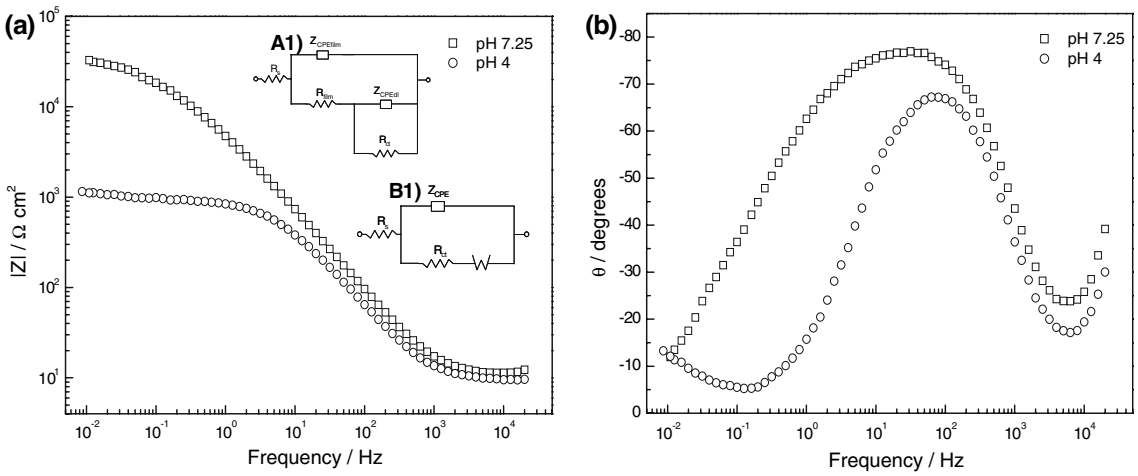

Fig. 6 EIS Bode diagrams for nickel immersed 24 h in aerated SBF at 37 °C at pH 7.25 and 4. (**a**) |Z| vs. Frequency, (**b**) θ vs. Frequency. In the insert: Equivalent electric circuit employed to model the impedance data of nickel. (A1) pH 7.25, (B1) pH 4

Table 4 Circuit parameters for nickel immersed in aerated SBF for 24 h at pH 7.25 and 4

	pH 7.25	pH 4
R_s (Ω cm^2)	10 ± 0.16	10 ± 0.08
Y_{0film} (Ω^{-1} cm^{-2} s^n)	3.42 × 10^{-5} ± 1.03 × 10^{-6}	5.85 × 10^{-5} ± 8.26 × 10^{-7}
n_{film}	0.89 ± 4.49 × 10^{-3}	0.87 ± 2.19 × 10^{-3}
R_{film} (Ω cm^2)	1.03 10^4 ± 2.96 × 10^3	843.5 ± 10.71
Y_{0dl} (Ω^{-1} cm^{-2} s^n)	5.40 10^{-5} ± 1.59 × 10^{-5}	–
n	0.52 ± 8.44 × 10^{-2}	–
R_{ct} (Ω cm^2)	2.74 × 10^4 ± 5.13 × 10^3	–
R_{DO} (Ω cm^2)	–	290.2 ± 84.39
n_D	–	0.31 ± 3.94 × 10^{-2}
T	–	15.02 ± 2.55

The equivalent circuits employed to model the system parameters at pH 7.25 and 4 are presented in as an insert in Fig. 6(A1, B1) respectively. The corresponding fitting results are given in Table 4.

In neutral SBF two close time constants are derived, as it can be observed in the change of slope in the Bode plot |Z| vs. frequency. The film resistance is high, although it does not have a marked passivating character. This is concluded from the almost constant drop of the phase angle at lower frequencies without reaching zero, which could be associated with a diffusion process through pores in the film [18].

At pH 4 there is active dissolution of the metal, though a diffusion process is still observed at lower frequencies. The superficial film is attacked by the aggressive environmental leading to a very porous surface where the controlling process is the diffusion of the electrolyte through these pores.

Iron

The EIS Bode diagrams for iron after 24 h of immersion in SBF at 37 °C at pH 7.25 and 4 are shown in Fig. 7. As in the case of nickel, the behaviour of the metal is remarkably different in each pH condition. The equivalent circuits employed to fit the system parameters at pH 7.25 and 4 are presented in Fig. 7(A1 and B1) respectively. The resulting fitting values are given in Table 5.

At pH 7.25, two time constants are observed from the change of slope in the Bode diagram |Z| vs. frequency, evidencing a non-protective porous layer of corrosion products [18]. Still, a diffusion process is observed at lower frequencies due to the circulation of the electrolyte to reach the metal surface. This diffusion does not constitute the main contribution to the total impedance of the system but only modifies the shape of the spectrum obtained. The resistance values indicate that the layer present in the iron

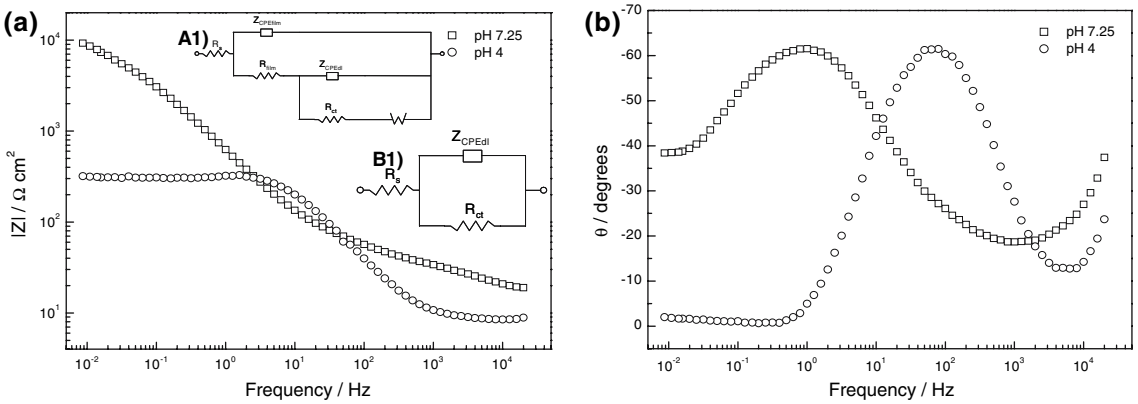

Fig. 7 EIS Bode diagrams for iron immersed 24 h in aerated SBF at 37 °C at pH 7.25 and 4. (**a**) |Z| vs. Frequency, (**b**) θ vs. Frequency. In the insert: Equivalent electric circuit employed to model the impedance data of iron. (A1) pH 7.25, (B1) pH 4

Table 5 Circuit parameters for iron immersed in aerated SBF for 24 h at pH 7.25 and 4

	pH 7.25	pH 4
R_s (Ω cm^2)	22 ± 0.79	22 ± 0.11
Y_{0film} (Ω^{-1} cm^{-2} s^n)	$1.34 \times 10^{-4} \pm 5.03 \times 10^{-5}$	–
n_{film}	$0.70 \pm 4.50 \times 10^{-2}$	–
R_{film} (Ω cm^2)	50.44 ± 7.51	–
Y_{0dl} (Ω^{-1} cm^{-2} s^n)	$2.67 \times 10^{-4} \pm 4.61 \times 10^{-5}$	$9.05 \times 10^{-5} \pm 2.77 \times 10^{-6}$
n	$0.78 \pm 2.32 \times 10^{-2}$	$0.88 \pm 4.85 \times 10^{-3}$
R_{ct} (Ω cm^2)	$1.04 \times 10^4 \pm 0.73 \times 10^3$	310.5 ± 2.24
R_{DO} (Ω cm^2)	$1.36 \times 10^4 \pm 1.51 \times 10^3$	–
n_D	$0.76 \pm 3.89 \times 10^{-2}$	–
T	67.28 ± 8.55	–

surface is much more porous and non-protective compared to the nickel one.

The behaviour observed at neutral pH conditions changes to a resistive behaviour under charge transfer control at pH 4. This is associated with a corrosion process that occurs in the metallic substrate, leading to active dissolution of the material.

With the aim to develop a more representative infected biological medium, other studies, including inoculation with *Staphylococcus epidermidis* in vitro and in vivo, as well as longer immersion time tests, are already in progress in order to consider the effect of the presence of bacteria in the corrosion behaviour of the material [19].

Conclusions

The corrosion potentials observed for each studied material were similar at pH 7.25 and pH 4 in the tested conditions. The nickel potential was the most similar to the AISI 316L stainless steel's one, while chromium and iron showed more negative values. This order of the E_{corr} was coincident with previous investigations of various stainless steels in different environments [11].

From the anodic potential curves at both pH conditions it is evident that chromium oxides have a major influence in the passive behaviour of the AISI 316L stainless steels in aerated SBF at 37 °C. However, the hysteretic loop observed in the stainless steel diagram is indicative that the performance of the material could be influenced by the presence of oxides from the other components of the alloy.

In infection conditions iron and nickel presented active dissolution behaviour and current densities one order of magnitude higher than chromium and the alloy. Therefore, it would be expected that under infection conditions these first components would react preferentially, releasing their corrosion products to the surrounding tissue.

The impedance results are consistent with the observed trends in the potentiodynamic tests. The only exception is observed with chromium, which presents a smaller resistance than the one expected considering its passive behaviour. This could be explained considering that during the acquisition of the anodic polarization curves the potential increases, shifting the material towards a passive condition with the growth of superficial chromium-oxides. In contrast, EIS tests are conducted near E_{corr}, where the morphology of the pure chromium could influence its

performance if these oxides do not cover completely the inhomogeneous and porous original surface of the metal.

As a general conclusion, AISI 316L does no present remarkable changes in its corrosion behaviour in infection conditions when compared with normal human body conditions after short periods of immersion.

Acknowledgments This work has been carried out thanks to the cooperation program between the Argentine Research Council for Science (CONICET) and the Spanish National Research Council (CSIC) and the support of the University of Mar del Plata-National Agency of Scientific Promotion of Argentina (PICTO 11338). The authors are grateful to Fidex S.A. for providing materials for this research.

References

1. J. B. PARK, *Biomaterials Science and Engineering* (Plenum Press, New York, 1984)
2. CH.-CH. SHIH, CH.-M. SHIH, Y.-Y. SU, L. H. J. SU, M.-S. CHANG and S.-J. LIN, *Corros. Sci.* **46** (2004) 427
3. I. GURAPPA, *Mater. Charact.* **49** (2002) 73
4. J. JACOBS, C. SILVERTON, N. HALLAB, A. SKIPOR, L. PATTERSON, J. BLACK and J. GALANTE, *Clin. Orthop. Relat. Res.* **358** (1999) 173
5. R. VENUGOPALAN and J. GAYDON, *A Review of Corrosion Behaviour of Surgical Implant Alloys* (Perkin Elmer Instruments: Princeton, 2001) p. 99
6. J. J. JACOBS, J. L. GILBERT and R. M. URBAN, *J. Joint Bone Surg.* **80**(2) (1998) 268
7. V. POPA, I. DEMETRESCU, E. VASILESCU, P. DROB, A. SANTANA LÓPEZ, J. MIRZA-ROSCA, C. VASILESCU and D. IONITA, *Electrochim. Acta* **49** (2004) 2113
8. D. A. Jones, *Principles and prevention of Corrosion* (McMillan Publishing Company, New York, 1992) p. 571
9. T. KOKUBO, H. KUSHITANI, S. SAKKA, T. KITSUGI and T. YAMAMURO, *J. Biomed. Mater. Res.* **24** (1990) 721
10. Zplot for Windows, Electrochem. Impedance Software Operating Manual, Part 1 (Scribner Ass. Inc. Southern Pines, NC, 1998)
11. J. OLEFJORD and C. R. CLAYTON, *ISIJ Int.* **31**(2) (1991) 134
12. I. OLEFJORD and B.-O. ELFSTROM, *Corrosion* **38**(1) (1982) 46
13. A. R. BROOKS, C. R. CLAYTON, K. DOSS and Y. C. LU, *J. Electrochem. Soc.* **133** (12) (1986) 2459
14. M. J. CARMEZIM, A. M. SIMOES, M. F. MONTEMOR and M. da CUNHA BELO, *Corros. Sci.* **47** (2005) 581
15. A. DURÁN, A. CONDE, A. GOMEZ COEDO, T. DORADO, C. GARCIA and S. CERÉ, *J. Mater. Chem.* **14** (2004) 2282
16. Y. OKAZAKI and E. GOTOH, *Biomaterials* **26** (2005) 11
17. G. W. WALTER, *Corros. Sci.* **26**(9) (1986) 681
18. M. METIKOS-HUKOVIC, E. TKALCEC, A. KWOKAL and J. PILJAC, *Surf. Coat. Tech.* **165**(1) (2003) 40
19. A. J. Van Der BORDEN, H. V. Van Der MEI and H. J. BUSSCHER, *Biomaterials* **26** (2005) 6731